Accepted Manuscript

International Journal of Humanoid Robotics

Article Title:	A Human Joint Torque Estimation Method for Elbow Exoskeleton Control
Author(s):	Xinwei Li, Su Liu, Ying Chang, Sujiao Li, Hongliu Yu
DOI:	10.1142/S0219843619500397
Received:	13 April 2019
Accepted:	13 November 2019
To be cited as:	Xinwei Li *et al.*, A Human Joint Torque Estimation Method for Elbow Exoskeleton Control, *International Journal of Humanoid Robotics*, doi: 10.1142/S0219843619500397
Link to final version:	https://doi.org/10.1142/S0219843619500397

A Human Joint Torque Estimation Method for Elbow Exoskeleton Control

Xinwei Li[a, d], Su Liu[a,d], Ying Chang[c,d] ,Sujiao Li[b,d], Hongliu Yu[*a,d]
[a]Institute of Rehabilitation Engineering and Technology
[b]Shanghai Engineering Research Center of Assistive Devices
[c]School of Medical Instrument and Food Engineering
[d]University of Shanghai for Science and Technology

Abstract

Exoskeleton for motion assistance has obtained more and more attention due to its advantages in rehabilitation and assistance for daily life. This research aimed to probe into the kinetic human-machine interaction between the operator's elbow joint torque and the output of exoskeleton. The human elbow joint torque estimation was obtained by back propagation (BP) neural network with physiological and physical input elements including shoulder posture, elbow joint related muscles activation, elbow joint position, and angular velocity. An elbow powered exoskeleton was developed to verify the validity of the human elbow joint torque estimation. The average correlation coefficient of estimated and measured 3 shoulder joint angles are 97.9%, 96.2%, and 98.1%, which show that estimated joint angles are consistent with the measured joint angle. The average RMSE between estimated elbow joint torque and measured values is about 0.143Nm. The experiment results proved that the proposed strategy had good performance in human joint torque estimation.

Keywords: elbow exoskeleton, joint torque estimation, shoulder posture, electromyography, BP neural network

Introduction

With the rapid improvement of robot kinematics, control theory, and biomedical technology, robotic exoskeleton has attracted the interest of many researchers from multiple research field[1]. In recent decades, the exoskeleton robot has been closely combined with clinical practice. The assistive exoskeleton could help recover the human's muscle force effectively[2]. As a novel rehabilitation medical method, exoskeleton robot had significant potential in rehabilitation training and assistance in daily life (ADL).[3,4]

The existing control strategies of exoskeleton can be divided into force interaction control[5], predefined movement control[6] and inverse dynamics control[7,8]. Huang Bo et al. proposed an admittance control scheme with force interface for physical human-robot interaction with human subject's intention motion as well as dynamic uncertainties of the robotic exoskeleton[9]. T. Mikolajczyk et al. made a point of 'Assistance-as-Needed' became a widely known control scheme of force interaction strategy for exoskeleton control[10], and then Y. Mao et al. proposed a threshold value force control for activating the exoskeletons[11]. The force interaction control performs well in human-machine interaction but failed to achieve good rehabilitation training effects in uniform passive motion compared with predefined movement control[12]. Di Ao et al. evaluating a movement performance of human-robot cooperation control with a predefined track for an ankle power-assist exoskeleton[13]. Inverse dynamics controls are widely applied in trail-pull exoskeletons for power assistance. Huang B et al. put up an admittance control scheme for physical human-robot interaction with human subject's intention motion as well as dynamic uncertainties of the robotic exoskeleton[9], which enables the human subjects to execute tasks on the exoskeleton robot effectively.

Based on the above discussions, the human body movement intentions recognition is necessary for exoskeleton control. The traditional movement intention recognitions are divided into physical and physiological based methods. In the traditional joint measurement, rotations can be estimated using optical motion capture, that method is largely limited to the laboratory and small capture volumes. These limitations may be overcome by developing wearable inertial measurement units (IMUs)[14,8]. Ong, Z et al. developed an economic and portable motion assessment system which involves wireless IMUs dedicated to study and assess body joints[15]. MA et al. investigated the accuracy of five different IMUs of the same type in measuring 3D orientation in static situations, as well as the calibration of the accelerometers and magnetometers within the IMUs[16].

The prediction of the operator's movement intention recognition for the powered assistive exoskeletons can also base on physiological signals, such as surface electromyography (sEMG)[17,18,19] signals and electroencephalography (EEG) signals. sEMG signals, which has been a mature technique, can reflect the levels of activation of muscles and are highly related to the muscle contraction force[20,21]. Moreover, in contraction of skeletal muscle, a delay exists between the onset of electrical activity and measurable tension[22]. This delay in electromechanical coupling has been stated to be between 30 and 100 ms. Thus, in rapid movements, it may be possible for sEMG activity to have terminated before force can be detected[23]. The main approaches of sEMG-based control have included classification algorithms, continuous proportional control and continuous non-linear control with or without a physiological model[13]. Tyler Desplenter et al. used seven classical muscle activation models in an optimization procedure to determine which model has the best performance in elbow motion estimation[24]. Longhai Lu et al. developed a joint torque estimation control strategy with sEMG from biceps to estimate the motion intention for a soft elbow exoskeleton to provide effective power assistance[25]. Suncheol Kwon et al. investigated the variation in human movement stability while the amount of sEMG-based assistive power was changed for elbow joint[26]. However, the performance of a continuous linear control strategy is not satisfying at yet, and the Hill-type-based non-linear control strategy requiring joint kinematics parameters are going to be simplified.

In our preliminary research on the relationship between sEMG signals and muscle force, no matter what kind of muscle activation models[24] referred by Tyler Desplenter are unstable due to the transformation of the upper limb posture. The feasibility of Hill-type neuromusculoskeletal models for the human-machine interface of powered assistive systems has been certified, however, few studies explored the movement performance of Hill-type models with quantitative analysis in comparison with other continuous control strategies. Here, we ponder the human joint torque estimation from another direction. The assistive torque of elbow exoskeleton was obtained by back propagation (BP) neural network with physiological and physical input signals. A single joint powered exoskeleton for an elbow was developed that could provide assistive torque for the operator to complete a series of rehabilitation tasks.

Methods

Power-Assist Exoskeleton Robot

The whole power-assist exoskeleton system consists of a customized actuated mechanical part, a self-designed multi-channel sEMG amplifier and a controller based on STM32F407ZGT6, a direct drive brushless DC servo motor (EC-i-52, Maxon, Switzerland) with a servo driver (EPOS4 Module 50/8, Maxon, Switzerland), a static discontinuous torque sensor (TJN-1, Tianguang Sensor Corporation, China), two high sensitive IMUs (LPMS-ME1, LP-RESEARCH In, Japan), a personal computer, a USB-serial port device and a Matlab-Opensim PC GUI program. The single joint powered exoskeleton was applied to assist elbow dorsiflexion, which is shown in Fig.1.

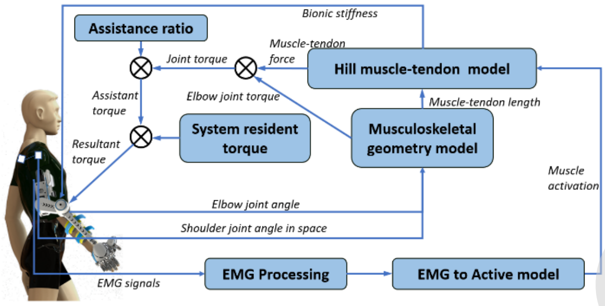

Fig.1.Control Diagram of the Elbow Rehabilitation System

In the wearable elbow exoskeleton system, the servo motor is connected to the actuated mechanical module to generate driving torque with double-stage deceleration. The upper arm forearm fixed mechanism can be flexible to suit the operator's different upper limb diameters. Each fixed mechanism also included the adjustable slots that could change the length of the arm. The 2 forearm fixed blocks can slide in a linear rail with restrictions of 3 springs which releases the degree of freedom of forearm in the direction of the linear rail. The movement of forearm ensures the centers of the joint of elbow exoskeleton the operator's elbow can be coincident continuously. A variable stiffness mechanism with a coil spring can improve bionic compliance and safety of physical human-robot interaction. The position and the stiffness of the flexible joint can be controlled by the main driving motor and the linear actuator respectively. The impact of the rigid gyration on the operator's elbow joint can also be buffered by the coil spring. The physical model of wearable elbow exoskeleton can be illustrated in Fig.2.

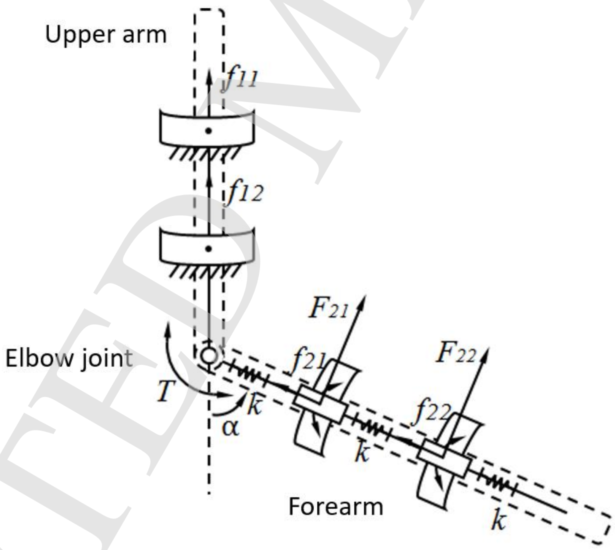

Fig.2.Physical Model of Elbow Exoskeleton

The main muscular contraction and extension of elbow movement are collected by sEMG electrodes which are attached to biceps brachii and triceps brachii. Afterward, the sEMG feedback signals amplified by the sEMG sensors are imported into the target computer through a 16-bit analog-to-digital conversion. Besides, the IMUs, attached to the upper arm and forearm of the operator, are connected to the self-designed board to calculate the elbow joint angle and the posture of the upper limb. The locomotion messages are also transmitted to the computer by serial communication. Then an sEMG-posture-based torque estimation control strategy developed based on neuromusculoskeletal models involving the kinematic, kinetic, and myoelectrical signals, is proposed for the elbow exoskeleton to provide assistance. The Matlab-OpenSim system has three functions: (1) running the sEMG-posture-based torque estimation control strategy, controlling actuator motor with servo driver and changing the stiffness of the exoskeleton joint with linear actuator; (2) graphically representing real-time signals about sEMG, elbow joint angle and posture of upper limb to guide the experiments; (3) holding sEMG, estimated joint torque, and joint angle motion and estimated posture signals for later analysis. The prototype of the elbow exoskeleton wore on a patient can be seen in Fig.3.

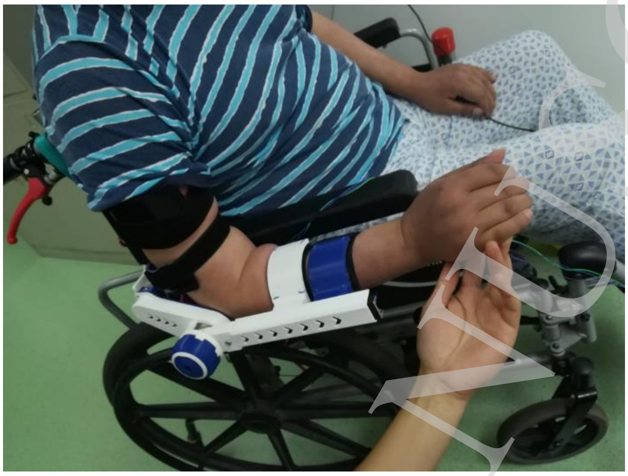

Fig.3.The prototype of elbow exoskeleton with a wearer

Multi-information Torque Estimation Control Strategy

For estimating joint torque in the motion intention, the sEMG signals representing the muscle activation level are collected and processed. The traditional approaches estimating joint torque from the sEMG signals are proposed to approximate the active state for a Hill-type muscle model[24]. Besides, the motion capture system is needed to acquire the accurate joint kinematics parameters for joint torque estimation. In this paper, the developed approach is capable of estimating joint torque with modeling processes and joint kinematics parameters for the Hill-type model. The elbow joint torque estimation control strategy fuses multi-information including shoulder posture, elbow joint angle, velocity and muscle activation of biceps brachii. Furthermore, this approach can be easily implemented for the developed soft exoskeleton suit and suitable for different users with a period of training time and classification.

1) Shoulder posture estimation

For the forward flexion angle of the upper arm is less than 90°, there is no gimbal lock in the estimation of shoulder posture. Thus, We use an existing method of biomechanical modeling based on a sequence of links connected by joints. These four parameters are known as the Denavit–Hartenberg (D-H) parameters[8,27] and will be specified for the shoulder in this section.

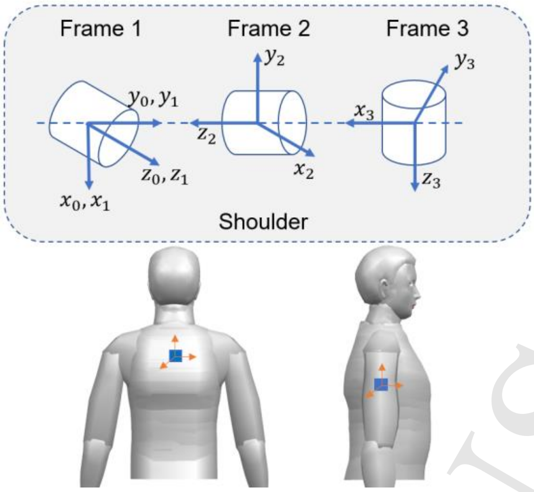

Fig.4.Structure of Hill-based muscle–tendon model

The model for the shoulder with three degrees of freedom (DOFs). Frames 1 through 3 represents shoulder flexion/extension, abduction/adduction, and internal/external rotation respectively as shown in Fig.3. The relative rotation of two IMUs can be transformed into the posture of the shoulder in three dimensions.

Table 1: D-H parameters for the shoulder model

Frame	a_{i-1}	α_{i-1}	d_i	θ_i
1	0	0	0	θ_1
2	$\pi/2$	0	0	$\theta_2+\pi/2$
3	$\pi/2$	0	l_{ul}	$\theta_3+\pi/2$

Table 1 shows the D-H parameters, where α_{i-1} is the rotation angle from frame $i-1$ to frame i making the two coordinate systems coincide, l_{ul} is the length of the upper arm, and θ_i is the angle i of rotation.

2) Evaluation of muscle activation

During the data acquisition, the sEMG signals from biceps collected by the sEMG sensor and amplified by a signal amplification circuit. In order to acquire the optimized signals, the sEMG sensors are put on the center of muscle and parallel to the direction of muscle fiber. The procedure of sEMG signals processing can be illustrated in Fig.4.

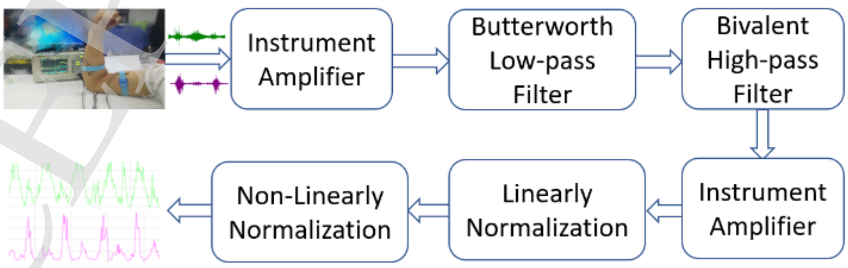

Fig.5.The procedure of sEMG singles processing

Muscle activation represents the neural inspiration of each muscle actuator which is an essential input to the Hill-type muscle model. The magnitude of the activation is related to the intensity of the muscular contraction. Consequently, the recorded sEMG can characterize muscle activation. The derivation from sEMG to muscle activation consists of 2 steps. Firstly, sEMG signals are transformed into intermediate variables as Eq.1.

$$e_i(t) = \mu_i s_i(t - de) - \kappa_i e_i(t-1) - \delta_i e_i(t-2) \tag{1}$$

where $e_i(t)$ is the intermediate processed sEMG related in a recursive manner to the filter sEMG for muscle i from time t to de, μ_i is a scale factor for muscle which is used to account for inter-subject differences in muscle parameters, de is an electromechanical delay and κ_i, δ_i are recursive coefficients. The sEMG-muscle-activation model we use is similar to the linear discrete-time dynamic model proposed by Thelen[28] but differs in accounting for non-linearities of sEMG to force relationship. Linear and non-linear relationships have been reported in previous research. In our work, the activation relationship above is modeled by the following function:

$$Act_i(t) = \frac{\left(\mathrm{e}^{A_i E_i(t)} - 1\right)}{\left(\mathrm{e}^{A_i} - 1\right)} \tag{2}$$

where $Act_i(t)$ is muscle activation for muscle i at time t and the A_i coefficient is a shaping factor specific to muscle i. The relationship between muscle activation to force is regulated by A_i.

Table 2 :Average Correlation r, RMS, and Maximum Error between IMUs and Optical Motion Capture System

Motion	RMSE/◦	Max error/◦
Elbow Flexion	1.5	0.6
Shoulder Flexion	3.5	1.0
Shoulder Abduction	2.4	0.8

3) sEMG-posture-based Torque Estimation Control Strategy

In this paper, in order to achieve better performance, the back propagation (BP) neural network, which is a kind of multi-layer feedforward network based on the error back propagation algorithm for training, is used to estimate the torque. The input layer of the BP neural network model is set to 4 layers, including the muscle activation, the angle and angular velocity of elbow flexion and the posture of the upper limb. The torque at the same moment is used as the output of the neural network. The hidden layer of BP neural network model is set to 10 layers, the transfer function of the first layer is tansig, and the transfer function of the second layer is purelin. The levenberg-marquardt algorithm is selected as the training function. Compared with other algorithms, it can achieve better results after training for a shorter time. The architecture of the neural network can illustrate sEMG-posture-based torque estimation as shown in Fig.5.

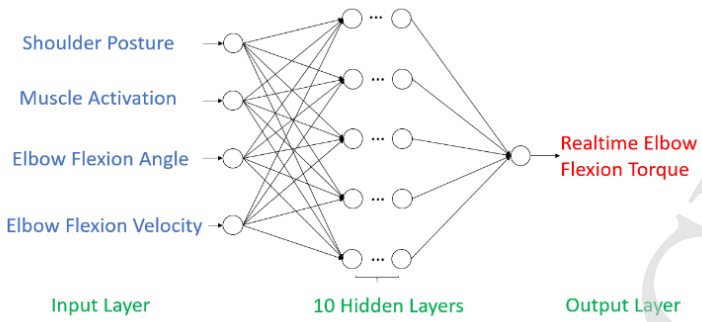

Fig.6.BP Neural Network Architecture

In the BP neural network training process, the errors between estimated and measured joint torque, mean square error (MSE) was considered, which is described as:

$$MSE = \frac{1}{T}\sum_{t=1}^{T}(T_{rt} - T_{et}) \tag{3}$$

where T_{rt} is the real torque of the elbow joint and T_{et} is the estimated value of it.

Experimental Setup

1) Volunteers selection

In this study, 10 healthy volunteers who had no muscle-skeleton disease (righthanded, 22.7 ± 2.1 years old, 5 males and 5 females). Before the experiments, the subjects wore the powered exoskeleton and fastened their upper arm and forearm in the dominant side to the supporter and the footplate, respectively. Characteristics of included volunteers are displayed in Table 3.

Table 3 Characteristics of Volunteers

Variables	Volunteers in the experiments(n=10)
Age(years)	22.7(20-24)
Sex(male/female)	5/5
Height(cm)	173(162-180)
Weight(kg)	62.1(52.3-75.8)

2) Motion tracking calibration

To evaluate the performance of the shoulder posture and elbow joint tracking system, we compared the joint angles calculated by the inertial tracker with those from an optical motion tracking system. We collected two datasets from a total of ten subjects performing tasks described in Table 3. The optical motion tracking recorded the position of 5 reflective markers placed on the upper arm, forearm, and shoulder. Analogously, elbow joint was obtained from the 3D positions of the markers placed on the upper arm and forearm based. Optical and inertial systems were synchronized to start and stop recording simultaneously. The IMUs data was originally sampled at 100Hz and the optical data at 60Hz. The angles calculated from IMUs were then transformed to 60Hz for comparison to the optical angles.

3) Real elbow joint torque measurement

In the elbow joint torque measurement, we designed a simplified method for the whole process as shown in Fig.6.

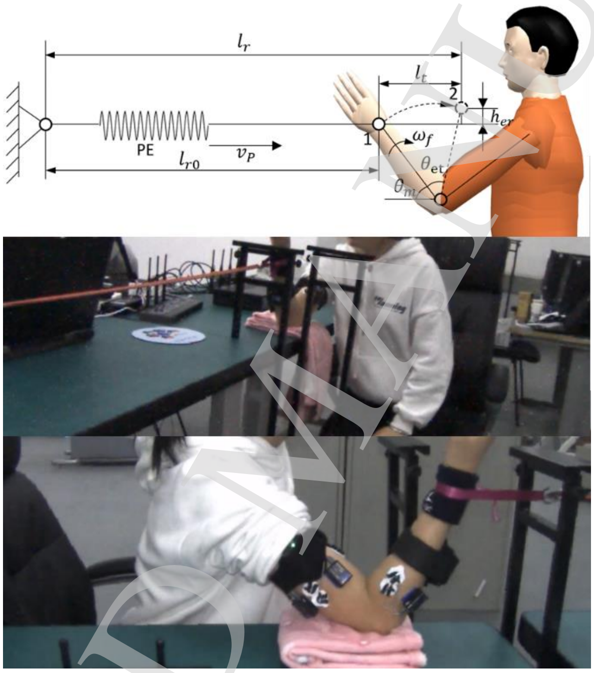

Fig.7.Elbow Joint Torque Measurement

The height deflection of volunteer's wrist h_{er} can be ignored if the length from position 1 of the wrist to the fixed side of the elastic string is long enough. Therefore, the trajectory of the wrist can be treated as a straight line which is parallel to the ground and the relative displacements is described as:

$$l_t = l_f[\cos\theta_m - \cos(\theta_m + \theta_{et})] \tag{4}$$

where l_f is the length of the forearm. Here we deemed that the elastic behaves according to Hooke's Law and its spring constant is $5N/cm$. The resilience starts from position 1 which means the force on the wrist is proportional to the displacement of it in the horizontal direction. Consequently, the elbow joint torque could be determined as follows according to the force equilibrium:

$$T_r = kl_f l_t \sin(\theta_{et} + \theta_{em}) \tag{5}$$

Results and Discussion

Shoulder posture estimation

To validate our shoulder kinematic models, used to generate the state and observation equations, we first investigate the performance of optical tracker on synthetic data generated by the shoulder posture estimation models. The root-mean-square error (RMSE) between the synthetic and estimated angles and was less than $3.5°$ for all 3 shoulder angles on average. Fig.7 shows the true (solid lines) and estimated (dotted lines) shoulder angles in 3 dimensions. The Frame 3 (shoulder internal rotation) behaved little undulation that could be omitted.

The experiment results of shoulder posture estimation are shown in Fig.7. In the contrast of estimated and measured joint angles in 3 dimensions with the same position, the average correlation coefficient, 97.90%, 96.2%, and 98.1%, show that estimated joint angles are consistent with the measured joint angle, and the average RMSE estimated and measured joint angle is about $1.632°$. The results of our workis correspond with Z. C. Ong's work on an economic wireless human motion analysis device for assessment of human body joint by the quaternion. However, there are still some errors especially in the period of holding maximum flexion and torque.

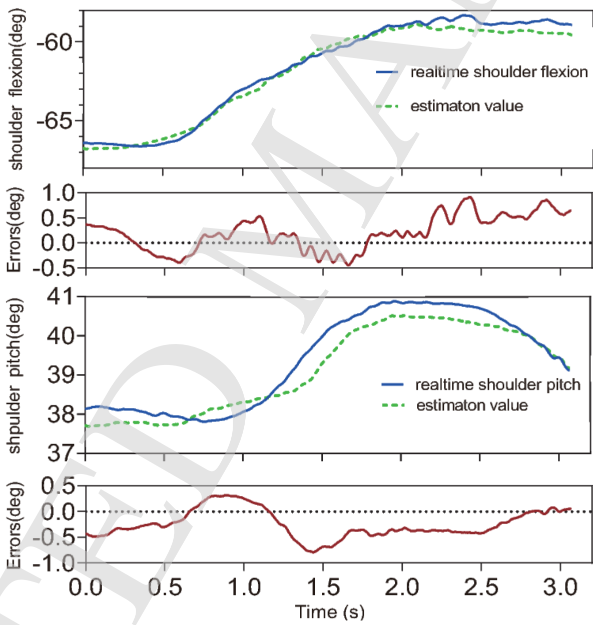

Fig.8.Shoulder Posture Estimation

Muscle activation

The average sEMG signals from biceps and triceps collected by 4 sEMG sensors. Bipolar sEMG signals need to be rectified and smoothed with a moving average or RMS algorithm with typically 50 to 100ms time constant and post-processed. Afterward, with a signal amplification circuit the processed results of average values of sEMG were analysed as shown in Fig.8. On the contrary of Suncheol Kwon's research on the variation in human movement stability with sEMG-based assistive power for elbow joint[26], the muscle activation reckoned by sEMG cannot fully represent the mechanical properties of human joint despite that the investigated subject is not changed as Lopez-Delis claimed[18].

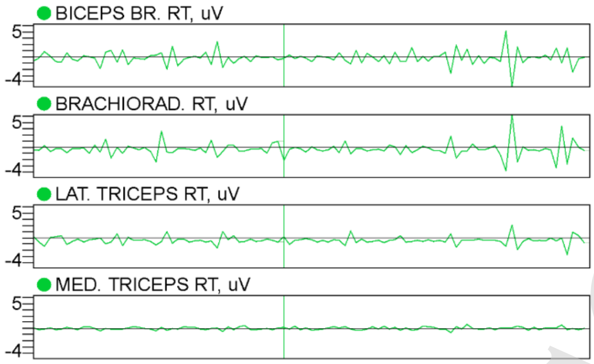

Fig.9.Muscle Activation of Biceps and Triceps

The averaging process detects the prototypical 'behavior' of muscle activation as the variability between single repetitions blends into an average pattern for the movement. This method of sEMG processing creates highly reproducible sEMG patterns. These patterns can be replicated for repeated measurements and serve as a basis for test-retest comparison plots.

The muscle activation modeled as Eq.2 of the whole experiment process was conducted as an input element for elbow joint torque estimation in the BP network.

Elbow joint torque estimation

Besides of the shoulder posture, biceps and triceps muscle activation, the other 2 input elements in the BP neural network, elbow joint angle and velocity, were collected by the rotary encoder which is coaxial with the joint of elbow exoskeleton. In order to avoid over-fitting, the BP neural network randomly divides the data set into a training set, a verification set, and a test set with a ratio of 3:1:1. The mean square error of the training set (blue line), the verification set (green line), and the test set (red line) in the iterative process are shown in Fig.9 and the network can be trained after a few iterations.

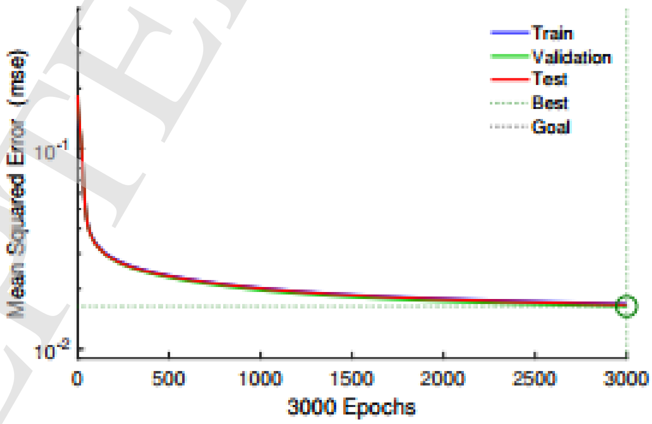

Fig.10.Best Validation Performance is 0.0012711 at epoch 5000

The comparison of estimated and measured joint torque of a subject during elbow joint movement in one period of motion is shown in Fig.10. The solid red line represents the estimated joint torque, and the solid blue line represents the real joint torque obtained by the change in the length of the spring.

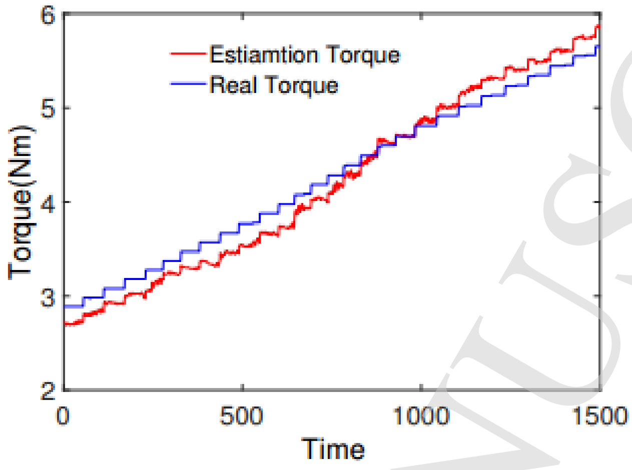

Fig.11.Torque Real Value and Estimation

The experiment results of elbow joint torque estimation are shown in Fig.11. By comparison of the estimated and measured elbow joint torque during the elbow flexion, the average correlation coefficient, 96.90%, shows that estimated joint torque is consistent with measured one, and the average RMSE estimated and measured joint torque is about $0.143Nm$.

The previous research on the relationship between sEMG signals and muscle force reveals that no matter what kind of muscle activation models[24] referred by Tyler Desplenter are unstable to estimate the joint torque and muscle force. The method proposed above proves that joint torque estimation with physiological and physical factors are more appropriate for human–exoskeleton interface. The powered-assistive elbow exoskeleton could provide continuous assistive torque for the operator to complete a series of rehabilitation tasks. The continuous near-liner loads applied to the estimation of assistive torques by the neuromusculoskeletal models, which differs from the previous research by Longhai Lu's research on a joint torque estimation control strategy with sEMG from biceps for a soft elbow exoskeleton to provide effective power assistance[25].

Limitations and future work

The continuous changing loads could be more close to the real application environment, however that made the off-line training of BP neural network cost longer time. For improving the response of the elbow exoskeleton, fuzzy mathematics and multi-input optimization will be applied to solve this problem and establish the BP model.

Conclusion

In this paper, a continuous multi-information-based torque estimation control strategy combining sEMG, IMUs and rotary encoder signals was researched and applied to the elbow exoskeleton. The methods were provided and discussed detailedly, and the corresponding experiments were conducted to verify the feasibility of means as well. Experiment results suggest that the proposed human joint torque estimation methods could be well utilized in the assistive torque calculated for elbow exoskeleton. Moreover, this strategy also could be potential in industrial exoskeleton for operation workers and the active rehabilitation training for patients after stroke. The experiments now available are conducted by healthy volunteers, the muscle activation processed methods must be more reliable to the weaken sEMG signals of patients with upper limb amyasthenia.

Acknowledgments

The authors gratefully acknowledge the financial supports by Shanghai Pujiang Program (16PJC063) and National Natural Science Foundation of China (61473193, 61803265).

Reference

[1] A.T. Asbeck, S.M.M. De Rossi, I. Galiana, Y. Ding, C.J. Walsh, Stronger, Smarter, Softer Next-Generation Wearable Robots, Ieee Robotics and Automation Magazine, 21 (2014) 22-33.

[2] K. Nasilowski, J. Awrejcewicz, and D. Lewandowski. Kinematic analysis of the finger exoskeleton using matlab/simulink.Acta of Bioengineering and Biomechanics,16(3):129–134, 2014.

[3] C. Irmscher, E. Woschke, E. May, and C. Daniel.Design, optimisation and testing of a compact, inexpensive elastic element for series elastic actuators. Medical Engineering and Physics, 52:84–89, 2018.

[4] Y. Liu, S. X. Guo, H. Hirata, H. Ishihara, and T. Tamiya. Development of a powered variablestiffness exoskeleton device for elbow rehabilitation. Biomedical Microdevices, 20(3), 2018.

[5] Justin Ghan, Ryan Steger, and H. Kazerooni. Control and system identification for the berkeley lower extremity exoskeleton (bleex). Advanced Robotics, 20(9):989–1014, 2006.

[6] Michael Wehner, Brendan Quinlivan, Patrick M. Aubin, Ernesto Martinez-Villalpando, Michael Baumann, Leia Stirling, Kenneth Holt, Robert Wood, Conor Walsh, and Ieee. A Lightweight Soft Exosuit for Gait Assistance, pages 3362–3369.IEEE International Conference on Robotics and Automation ICRA. 2013.

[7] Ye Ding, Ignacio Galiana, Alan T. Asbeck, Stefano Marco, Maria De Rossi, Jaehyun Bae, Thiago Ribeiro Teles Santos, Vanessa Lara de Araujo, Sangjun Lee, Kenneth G. Holt, and Conor Walsh. Biomechanical and physiological evaluation of multi-joint assistance with soft exosuits. Ieee Transactions on Neural Systems and Rehabilitation Engineering, 25(2):119–130, 2017.

[8] J. Favre, B. M. Jolles, O. Siegrist, and K. Aminian. Quaternion-based fusion of gyroscopes and accelerometers to improve 3d angle measurement. Electronics Letters, 42(11):612–614, 2006.

[9] B. Huang, Z. Ye, Z. Li, W. Yuan, and C. Yang.Admittance control of a robotic exoskeleton for physical human robot interaction. In 2017 2nd International Conference on Advanced Robotics and Mechatronics (ICARM), pages 245–250, 2017.

[10] T. Mikolajczyk, A. Klodowski, E. Mikoltajewska, P. Walkowiak, P. Berjano, J. H. Villafane, F. Aggogeri, A. Borboni, D. Fausti, and G. Petrogalli. Design and control of system for elbow rehabilitation: Preliminary findings. Advances in Clinical and Experimental Medicine, 27(12):1661–1669, 2018.

[11] Y. Mao and S. K. Agrawal. Design of a cable-driven arm exoskeleton (carex) for neural rehabilitation. IEEE Transactions on Robotics, 28(4):922–931, Aug 2012.

[12] Hsien-Ting Chang, Li-Wei Cheng, and JenYuan Chang. Development of IMU-Based Angle Measurement System for Finger Rehabilitation. Proceedings of 2016 23rd International Conference on Mechatronics and Machine Vision in Practice. 2016.

[13] Di Ao, Rong Song, and Jinwu Gao. Movement performance of human-robot cooperation control based on emg-driven hill-type and proportional models for an ankle power-assist exoskeleton robot. Ieee Transactions on Neural Systems and Rehabilitation Engineering, 25(8):1125–1134, 2017.

[14] R. V. Vitali, S. M. Cain, R. S. McGinnis, A. M.
Zaferiou, L. V. Ojeda, S. P. Davidson, and N. C. Perkins. Method for estimating threedimensional knee rotations using two inertial measurement units: Validation with a coordinate measurement machine. Sensors, 17(9):16,2017.

[15] Z. C. Ong, Y. C. Seet, S. Y. Khoo, and S. Noroozi.
Development of an economic wireless human motion analysis device for quantitative assessment of human body joint. Measurement, 115:306–315, 2018.

[16] M. A. Brodie, A. Walmsley, and W. Page. The static accuracy and calibration of inertial measurement units for 3d orientation. Computer Methods in Biomechanics and Biomedical Engineering, 11(6):641–648, 2008.

[17] Zhijun Li, Baocheng Wang, Fuchun Sun, Chenguang Yang, Qing Xie, and Weidong Zhang. semg-based joint force control for an upperlimb power-assist exoskeleton robot. Ieee Journal of Biomedical and Health Informatics, 18(3):1043–1050, 2014.

[18] A. Lopez-Delis, D. Delisle-Rodriguez, A. C. Villa-Parra, T. Bastos-Filho, and Ieee. Knee Motion Pattern Classification from Trunk Muscle Based on sEMG Signals, pages 2604–2607. IEEE Engineering in Medicine and Biology Society Conference Proceedings. 2015.

[19] Christian Fleischer and Guenter Hommel. A human-exoskeleton interface utilizing electromyography. Ieee Transactions on Robotics, 24(4):872–882, 2008.

[20] Tommaso Lenzi, Stefano Marco Maria De Rossi,
Nicola Vitiello, and Maria Chiara Carrozza.Intention-based emg control for powered exoskeletons. Ieee Transactions on Biomedical Engineering, 59(8):2180–2190, 2012.

[21] B. Hudgins, P. Parker, and R. N. Scott. A new strategy for multifunction myoelectric control. Ieee Transactions on Biomedical Engineering,40(1):82–94, 1993.

[22] Francois Hug, Thomas Gallot, Stefan Catheline, and Antoine Nordez. Electromechanical delay in biceps brachii assessed by ultrafast ultrasonography. Muscle and Nerve, 43(3):441–443,2011.

[23] P V Cavanagh, P R; Komi. Electromechanical delay in human skeletal muscle under concentric and eccentric contractions. European journal of applied physiology and occupational physiology, 1979.

[24] T. Desplenter and A. L. Trejos. Evaluating muscle activation models for elbow motion estimation. Sensors, 18(4):19, 2018.

[25] L. H. Lu, Q. C. Wu, X. Chen, Z. Y. Shao, B. Chen, and H. T. Wu. Development of a semg-based torque estimation control strategy for a soft elbow exoskeleton. Robotics and Autonomous Systems, 111:88–98, 2019.

[26] Suncheol Kwon, Yunjoo Kim, and Jung Kim. Movement stability analysis of surface electromyography-based elbow power assistance. Ieee Transactions on Biomedical Engineering, 61(4):1134–1142, 2014.

[27] M. El-Gohary and J. McNames. Shoulder and elbow joint angle tracking with inertial sensors. IEEE Transactions on Biomedical Engineering, 59(9):2635 2641, Sep. 2012.

[28] Kurt Manal, Roger V. Gonzalez, David G. Lloyd, and Thomas S. Buchanan. A real-time emg-driven virtual arm. Computers in Biology and Medicine, 32(1):25 – 36, 2002.